

Variational RVB wave function for the spin-1/2 Heisenberg Model on honeycomb lattice

Zahra Nourbakhsh*,¹ Farhad Shahbazi†,¹ S. A. Jafari‡,¹ and G. Baskaran²

¹Dept. of Physics, Isfahan University of Technology, 84156-83111, Isfahan, Iran

²Institute of Mathematical Sciences, Chennai 600113, India

(Dated: November 9, 2018)

In this work, a long-range resonating valence bond state is proposed as a variational wave function for the ground state of the $S = 1/2$ antiferromagnetic Heisenberg model on the honeycomb lattice. Employing Variational Monte Carlo (VMC) method, we show that the ground state energy obtained from such RVB wave function, lies well below the energy of the Néel state and compares very well to the energies evaluated from spin-wave theory and series expansion method. We also obtain the spin-spin correlation function along zig-zag and armchair directions and find that the two correlations are different, which indicates the anisotropic nature of the system. We compare our results with the square lattice and we show that although the quantum fluctuations on honeycomb lattice are much stronger, but do completely not destroy the magnetic order.

PACS numbers: 75.10.Jm, 75.50.Ee

Introduction: The resonating valence bond (RVB) state was originally proposed by Anderson and Fazekas as a possible ground state for the $S = 1/2$ Heisenberg spins with nearest neighbor anti-ferromagnetic coupling on triangular lattice [1, 2]. They found that for anisotropic Heisenberg model, near the Ising limit, the liquid-like RVB state is energetically more favorable than the Néel state. In such a state the $S = 1/2$ atoms residing on the lattice points, form singlet valence bonds in pairs and so lose some of their anti-ferromagnetic exchange energy with respect to the Néel order. In order to regain some of the lost exchange energy, they have to resonate quantum mechanically among many different pairing configurations. These states form the basis of Pauling's early theories of aromatic molecules such as benzene [3], however his theory was unable to give a proper description of the metallic state. The idea that the RVB state of spin-liquid type may give a precise picture of the two dimensional quantum anti-ferromagnet was once the most attractive topic after the discovery of the high- T_c superconductivity, when Anderson [4] suggested that an RVB state naturally leads to incipient superconductivity from preformed singlet pairs in the parent insulating state.

The anti-ferromagnetic Heisenberg model arises naturally in a Mott insulator, in which a system with an odd number of electrons per unit cell is insulating due to the strong Coulomb repulsion between two electrons on the same site (U). In such systems the kinetic exchange mechanism due to virtual hopping between anti-parallel spin configurations leads to anti-ferromagnetic exchange $J = 4t^2/U$ between the spins, where t is the hopping integral [5]. For $S = 1/2$ and in low dimensions, strong quantum fluctuations make the RVB liquid more favorable than the classically ordered Néel state. RVB is a fair description of anti-ferromagnetic Heisenberg linear chain, where there is no long-range order according to the

exact Bethe's solution [6]. The $S = 1/2$ anti-ferromagnet Heisenberg model on square lattice has been extensively studied [7] and it has been established that there is a Néel order in the system, although the quantum fluctuations reduce the staggered magnetization with respect to its classical value.

Apart from the fabrication of Graphene sheets which brought the honeycomb structure to the focus of condensed matter community, the recent discovery of compounds such as $\text{InCu}_{2/3}\text{V}_{1/3}\text{O}_3$ [8] in which the Cu^{+2} ions in the copper-oxide layers form a two-dimensional $S = 1/2$ anti-ferromagnet Heisenberg on a honeycomb lattice are our motivations for this study. Also the recent progress in the field of ultracold atoms and trapping techniques [9] along with the ability to tune the interaction parameters via the Feshbach resonance [10] can be thought of another way to realize Heisenberg spins (of localized fermions) on a honeycomb optical lattice.

In this work, we study the $S = 1/2$ Heisenberg spins with nearest-neighbor anti-ferromagnetic interactions on the honeycomb lattice. The number of nearest neighbors in honeycomb lattice equals 3, which is less than 4 of the square lattice, leading to enhancement of quantum fluctuations. This suggests that the RVB state could be a better variational wave function for honeycomb than the square lattice. In this work we choose the variational RVB wave function proposed by Liang, Doucot and Anderson in the context of HTSC cuprates [11] and show that RVB ansatz in honeycomb lattice gives very good results for the ground state energy by comparing with other methods.

Numerical calculation: Consider a system of atoms with $S = 1/2$ on a honeycomb lattice, consisting of two interpenetrating bravais sublattices (Fig. 1). The Heisenberg Hamiltonian with anti-ferromagnetic nearest neighbor interactions for this system is given by:

$$H = J \sum_{\langle i,j \rangle} \mathbf{S}_i \cdot \mathbf{S}_j, \quad (1)$$

where $J > 0$ and $\langle i,j \rangle$ denotes the nearest neighbors. Since the ground state of such Hamiltonian is a spin singlet [12], we

*Electronic address: z.nourbakhsh@ph.iut.ac.ir

†Electronic address: shahbazi@cc.iut.ac.ir

‡Electronic address: sa.jafari@cc.iut.ac.ir

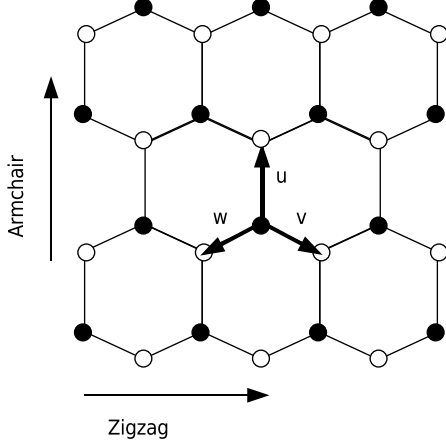


FIG. 1: Honeycomb lattice as a superposition of two simple monoclinic Bravais lattices denoted by filled and empty circles.

employ a RVB state as trial wave function. After its optimization, we calculate the ground state properties. The RVB trial wave function can be considered as summation over the all possible singlet pairings between each spin in one sublattice (say A) to spins on the other sublattice (B). Therefore the trial wave function is given by:

$$|\Psi\rangle = \sum_{\substack{i\alpha \in A \\ j\beta \in B}} h(i_1 - j_1) \dots h(i_n - j_n) (i_1, j_1) \dots (i_n, j_n) \\ = \sum_i w(c_i) |c_i\rangle \quad (2)$$

Where (i, j) represent a singlet bond. Denoting spin up state ($|\uparrow\rangle$) by α and spin down state ($|\downarrow\rangle$) by β , it can be expressed as:

$$(i, j) = \frac{1}{\sqrt{2}} (\alpha_i \beta_j - \beta_i \alpha_j). \quad (3)$$

In Eq. (2), $|c\rangle$ stands for a valence bond configuration which can be represented by:

$$|c\rangle = \prod_{a=1}^n (i_a, j_a). \quad (4)$$

The weight of a configuration $|c\rangle$ of valence bonds is given by

$$w(c) = \prod_{a=1}^n h(i_a - j_a), \quad (5)$$

where h is a pairing function describing a singlet bond as a function of bond length.

This wave function contains the two limiting cases of the nearest-neighbor RVB liquid (when $h(l) = 0$ for $l > 1$) and the Néel state (for which $h(l)$ is independent of the bond length). Sutherland derived a set of simple rules for estimating $\langle c_1 | \mathbf{S}_i \cdot \mathbf{S}_j | c_2 \rangle$ [13]. It is easy to show that the overlap between two configurations $|c_1\rangle$ and $|c_2\rangle$ is given by

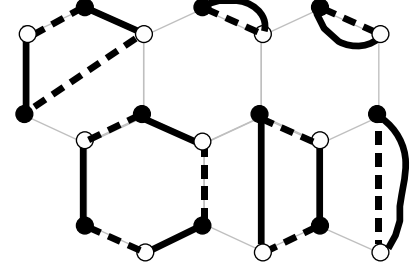


FIG. 2: The loop covering $\langle c_1 | c_2 \rangle$ is the superposition of $|c_1\rangle$ (solid line) and $|c_2\rangle$ (dashed line) on a honeycomb lattice. $|c_1\rangle$ and $|c_2\rangle$ are two singlet valence bond configurations with equal weight factors. In this example, there are six loops.

$\langle c_1 | c_2 \rangle = 2^{N(c_1, c_2)}$, where $N(c_1, c_2)$ is the number of loops in the overlap of the two configurations (Fig. 2). To compute the ground state energy as well as the spin-spin correlation functions, we use the following rules for the matrix elements of the Hamiltonian: (i) $\langle c_1 | \mathbf{S}_i \cdot \mathbf{S}_j | c_2 \rangle = 0$, if i and j belong to two different loops; (ii) $\langle c_1 | \mathbf{S}_i \cdot \mathbf{S}_j | c_2 \rangle = \pm \frac{3}{4} \langle c_1 | c_2 \rangle$, if i and j belong to the same loop, with a minus sign when i and j belong to two different sublattices, and a plus sign otherwise.

Using the wave function (2) along with the Hamiltonian (1), the ground state energy is given by:

$$E = \frac{\langle \Psi | H | \Psi \rangle}{\langle \Psi | \Psi \rangle} \\ = \sum_{c_1, c_2} \frac{w(c_1) w(c_2) \langle c_1 | c_2 \rangle}{\langle \Psi | \Psi \rangle} \times \frac{\langle c_1 | H | c_2 \rangle}{\langle c_1 | c_2 \rangle} \\ = \sum_{c_1, c_2} P(c_1, c_2) \times E(c_1, c_2), \quad (6)$$

in which $E(c_1, c_2)$ is the contribution in the ground states energy arising from the overlap of configurations $|c_1\rangle$ and $|c_2\rangle$ with the weight $P(c_1, c_2) = \frac{w(c_1) w(c_2) \langle c_1 | c_2 \rangle}{\langle \Psi | \Psi \rangle}$. Such overlaps can be graphically represented by loop coverings depicted in Fig. 2 [14]. The number of terms in this expression diverges exponentially with the system size, making the exact evaluation of the summation impossible. To overcome this difficulty, we use Monte Carlo approach based on important sampling for evaluating the ground state energy and also the spin-spin correlations. since $P(c_1, c_2)$ is positive, here there is no minus sign problem, and the Monte Carlo estimates can be made very precise.

Consider two configurations c_1 and c_2 with a given loop coverage. Using the standard Metropolis algorithm, loop configurations are updated by randomly choosing a couple of sites and exchanging their end point connections with a probability that satisfies the detailed balance condition [11]. The matrix elements are evaluated according to Sutherland's rule, once the loop covering associated with the two configurations is

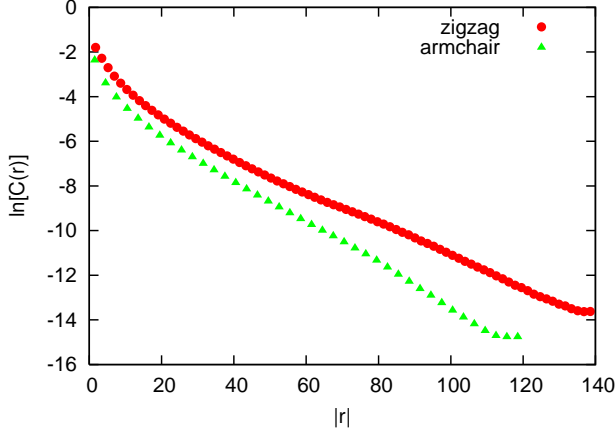


FIG. 3: The spin-spin correlation as a function of distance for the state labeled (1, 3, 5). See the text for explanations of the state. Circles denote zigzag direction data and triangles denote armchair data.

known. In our calculations, boundary conditions are taken to be periodic. The equilibrium state does not depend on the initial state, but in order to reach the equilibrium distribution faster, we started with a dimer state. In following we discuss our results for short-range and long-range RVB states.

Short-range RVB wave function: First we consider some wave functions with short singlet bonds. One example of this type is the nearest-neighbor RVB (NNRVB) trial wave functions for which $h(1) = 1$ and $h(l) = 0$ for larger distances $l > 1$. We choose l to be the Manhattan distance defined for two points separated by a vector $n_u \mathbf{u} + n_v \mathbf{v}$ in Fig. 1 by $l = |n_u| + |n_v|$. Defining $a_l = \frac{h(2l+1)}{h(2l-1)}$, we investigate other examples such as (1, 3) state with one variational parameter $a_1 = \frac{h(3)}{h(1)}$ and $a_l = 0$ for $l > 2$; (1, 3, 5) state with two variational parameters $a_1 = \frac{h(3)}{h(1)}$, $a_2 = \frac{h(5)}{h(3)}$; and exponential state for which $h(l)$ decays exponentially for large distances. In this state we have three variational parameters a_1, a_2 and $a_l = \text{const.}$ for $l \geq 2$. Among the short range states, the exponential state has lowest energy (see Table I). The statistical error in evaluation of energy from Monte Carlo calculation is 0.0002 and we check that the finite-size effects are less than this error. We have also computed the spin-spin correlation function defined as:

$$C_{ij} = \sum_{c_1, c_2} P(c_1, c_2) \frac{\langle c_1 | \mathbf{S}_i \cdot \mathbf{S}_j | c_2 \rangle}{\langle c_1 | c_2 \rangle}, \quad (7)$$

which results in exponentially decaying of the correlation at large distances, indicating the absence of long-range order for this variational states (Fig. 3). As it can be seen in Fig. 3, the correlation length along zigzag direction is larger than armchair direction. The correlation lengths ξ in units of the lattice spacing are listed in Table I.

Long-range wave functions: Next we study spin-spin correlations and energy for the class of wave functions which behave like $h(l) \propto l^{-p}$ in long distances. To optimize the en-

| State | $\frac{-E_0}{J}$ | ξ | $h(l)$ |
|-------------|------------------|----------------|--|
| NNRVB | 0.4310(2) | $\xi_a = 0.84$ | $h(1) = 1$ |
| | | $\xi_z = 1$ | $h(l) = 0, l > 1$ |
| (1, 3) | 0.5087(2) | $\xi_a = 4.7$ | $a_1 = \frac{2}{9}$ |
| | | $\xi_z = 5.9$ | $a_l = 0, l > 1$ |
| (1, 3, 5) | 0.5319(2) | $\xi_a = 9.55$ | $(a_1, a_2) = (\frac{1}{9}, \frac{2}{3})$ |
| | | $\xi_z = 11.1$ | $h(l) = 0, l > 2$ |
| Exponential | 0.5437(2) | — | $(a_1, a_2) = (\frac{2}{21}, \frac{1}{4})$ |
| | | — | $a_l = 0.32, l > 3$ |

TABLE I: Ground state energy, spin-spin correlation length and optimized parameters for the short ranged RVB states. The subscripts a, z stand for armchair and zigzag directions, respectively.

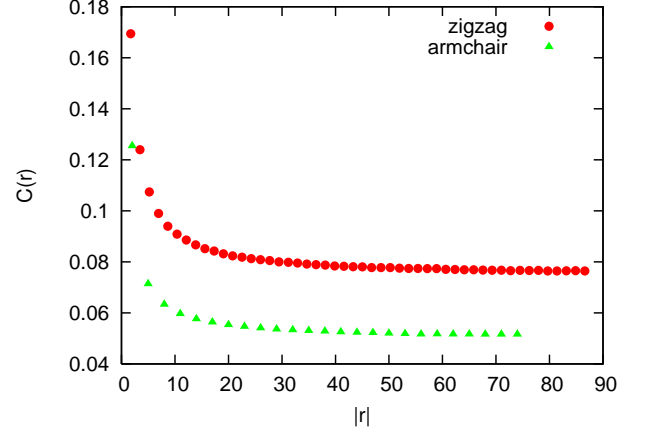


FIG. 4: spin-spin correlation as a function of distance for the states with algebraically decaying states with $p = 3$ (see the text), versus r along the zigzag (circle) and armchair (triangle) directions.

ergy, we choose $a_1 = \frac{h(3)}{h(1)}$, $a_3 = \frac{h(5)}{h(3)}$ as variational parameters and optimize them for various exponents p defined by $h(l) = h(5)(5/l)^p$ for $l > 5$. For long-bond singlets the spin-spin correlation function does not vanish at large distances and so the staggered magnetization can be determined from the tails of the correlation function. Because of the anisotropic nature of the honeycomb lattice, the correlations along zigzag and armchair directions are different hence we define the magnetization by

$$M^s = \sqrt{\lim_{r \rightarrow L/2} \frac{C_{\text{zigzag}}(r) + C_{\text{armchair}}(r)}{2}}, \quad (8)$$

where L is the linear size of the system.

| p | $\frac{-E_0}{J}$ | M_s | (a_1, a_2) |
|-----|------------------|---------|-------------------------------|
| 2 | 0.5434(2) | 0.30(2) | $(\frac{1}{16}, \frac{2}{9})$ |
| 2.5 | 0.5440(2) | 0.26(2) | $(\frac{2}{23}, \frac{2}{9})$ |
| 3 | 0.5438(2) | 0.25(2) | $(\frac{1}{19}, \frac{1}{4})$ |
| 3.5 | 0.5431(2) | 0.20(2) | $(\frac{1}{9}, \frac{1}{4})$ |
| 4 | 0.5430(2) | 0.19(2) | $(\frac{1}{8}, \frac{1}{7})$ |

TABLE II: Ground state energy, staggered magnetization and optimized parameters for the long ranged RVB states.

The optimal values for the parameters as well as ground state energies and staggered magnetizations within this class of states are listed in Table II for various values $p = 2, 2.5, 3, 3.5$ and 4 . For this set of exponents, we found that energy is minimum for $p = 2.5$ with $E_o = -0.5440J \pm 0.0002J$, which is lower than the energy of the short ranged RVB states. The staggered magnetization for $p = 2, 2.5, 3, 3.5$ and 4 are %60, %52, %50, %40, and %38 of Néel state, respectively. The magnetization decreases when p increases and seems to disappear when $p > 4$.

Conclusion: In summary, we presented a variational Monte Carlo estimate of the ground state energy for the $S = 1/2$ AF Heisenberg model on honeycomb lattice employing both short-range and long-range RVB trial wave functions. Similar to square lattice [11], we found that the long-bond wave functions give a better description of the ground state in honeycomb lattice. The optimized values of ground state energy and staggered magnetization are $E_o/J = -0.5440 \pm 0.0002$ and $M^s = 0.26$, respectively. The ratio of the RVB ground state energy to the Néel state energy is $\frac{E_{RVB}}{E_N} = \frac{0.5540}{0.375} = 1.48$, so RVB energy is %48 less than the Néel state. In square lattice, this ratio is %34, which can be justified in terms of stronger quantum fluctuation in honeycomb lattice due to its smaller coordination number. The quantum fluctuations also reduce the order parameter by about %50 with respect to classical Néel order.

Our results are in excellent agreement with other numerical methods, such as the series expansion [15] which gives the ground state energy $\frac{E_o}{J} = -0.5443 \pm 0.0003$ and magnetization $M^s = 0.266 \pm 0.009$ as well as spin wave calculation in first approximation with $\frac{E_o}{J} = -0.5324$ and $M^s = 0.2418$ and in second approximation with $\frac{E_o}{J} = -0.5489$ and $M^s = 0.2418$ [16]. This shows that RVB picture captures the main properties of the ground state for the AF Heisenberg model on the honeycomb lattice with higher precision than square lattice, leading to the conclusion that the stronger are quantum fluctuations, the more favorable is the RVB ground state. Therefore it seems that the RVB state is a good candidate for the ground state of the AF Heisenberg model on the honeycomb lattice. One can take a long ranged RVB as a reference starting point to proceed with the calculations of excitation energies [17]. Including charge fluctuations in such an RVB

state by adding hopping of underlying electrons has also been investigated [18, 19]. This view point can be taken as a possible route to describe the Dirac liquid semi-metallic in terms of RVB wave functions [20].

Acknowledgments: F.S. and S.A.J. thank the Abdus Salam ICTP for the hospitality during a short term summer visit, where some part of this work was done. S.A.J. was supported by ALAVI group Ltd. We thank H. Mosadeq for useful discussions.

-
- [1] P. W. Anderson, *Matt. Res. Bull.* **8**, 153 (1973).
 - [2] P. Fazekas, and P.W. Anderson, *Phil. Mag.* **30**, 432 (1974).
 - [3] L. Pauling, *The Nature of the Chemical Bond*, Cornell Univ. Press (1963).
 - [4] P. W. Anderson, *Science* **235**, 1196 (1987).
 - [5] P. W. Anderson, *Phys. Rev.* **115**, 2 (1959).
 - [6] H. A. Bethe, *Z. Phys.* **71**, 205 (1931).
 - [7] E. Manousakis, *Rev. Mod. Phys.* **63**, 1 (1991).
 - [8] V. Kataeva, A. Moller, U. Low, W. Junge, N. Schittner, M. Kriener and A. Freimuth, *J. Magn. Magn. Mater* **290-291**, 310 (2005).
 - [9] S. Aubin, S. Myrskog, M. H. T. Extavour, L. J. LeBlanc, D. McKay, A. Stummer, and J. H. Thywissen, *Nature Phys.* **2**, 384 (2006).
 - [10] S. Inouye, M. R. Andrews, J. Stenger, H. J. Miesner, D. M. Stamper-Kurn, and W. Ketterle, *Nature* **392**, 151 (1998).
 - [11] S. Liang, B. Doucot and P. W. Anderson, *Phys. Rev. Lett.* **61**, 365 (1988).
 - [12] W. Marshall, *Proc. Roy. Soc. (London)* **A232**, 48 (1955).
 - [13] B. Sutherland, *Phys. Rev. B* **47**, 5849 (1988).
 - [14] See chap. 6 of E. Fradkin, *Field Theories of Condensed Matter Systems*, Addison Wesley, 1991.
 - [15] J. Oitmaa, C. J. Hamer and Zheng Weihong, *Phys. Rev. B* **45**, 9834 (1992).
 - [16] Zheng Weihong, J. Oitmaa and C. J. Hamer *Phys. Rev. B* **44**, 11869 (1991).
 - [17] H. Mosadeq, *et al.*, in preparation.
 - [18] S. A. Jafari, arXiv: 0809.1109 (2008)
 - [19] S. Pathak, V. B. Shenoy, and G. Baskaran, arXiv: 0809.0244 (2008)
 - [20] G. Baskaran, S.A. Jafari, *Phys. Rev. Lett.* **89**, 016402 (2002).